Analysis of the plastic zone near the crack tips under the uniaxial tension using ordinary state-based peridynamics

X.P. Zhou

Y.D. Shou

F. Berto

Abstract

In this paper, the plastic model of ordinary state-based peridynamics is established. The size and shape of plastic zone around crack tips with the different inclination angles are simulated using ordinary state-based peridynamics. Comparison of the size and shape of plastic zone around the crack tips obtained from peridynamic solution and analytic solution is made. It is found that the relative errors between the analytical and peridynamic solution are very little. Therefore, it is feasible to predict the plastic zone around crack tips using ordinary state-based peridynamics.

1 INTRODUCTION

Fracture is one of the main damage forms in rock engineering and mechanical engineering. Especially, initiation and propagation of cracks are a hot issue in rock engineering. Actually, rocks can be divided into brittle rocks and ductile rocks (or hard rocks and soft rocks). Although the plastic zones around crack tips are quite small in the brittle rocks, the plastic zones around crack tips should not be ignored in ductile rocks, which has significant influence on crack propagation. In this study, the plastic zones around crack tips in ductile rock are focused. For the propagation of cracks, the size of plastic zone near the crack tip is considered as a measure of rock resistance against the driving force, and it plays an important role in determining initiation and propagation of cracks.[1-7] Therefore, it is important to know the exact size and shape of plastic zone around crack tips in rocks under loading. The earliest theoretical works on plastic zone shape around crack tips were provided by Irwin[8] and Dugdale.[9] Harmain and Provan[10] also predicted plastic zone shape around the tips of a mode I crack in isotropic materials using Tresca criterion under plane stress and strain conditions. Banks and Garlick[11] and Guerra-Rosa et al[12] analytically predicted the plastic zone boundary or locus under plane stress and plane strain conditions using the Mises yield criterion. Based on Mises and Tresca yield criterion, Benrahou et al[13]estimated the size of the plastic zone around the tips of mode I crack using the finite element method. Based on the unified strength theory, the unified solution of the shapes and sizes of

plastic zone around modes I crack tips under small-scale yielding was obtained by Qiang et al[14] and Zhang et al,[15] respectively. Gao et al[16] studied the plastic zone around crack tips under various loading conditions and obtained some characteristics of the plastic zone around crack tips. They found that the plastic zones around crack tips present “butterfly-like” shape and the size of the plastic zone is largest for pure mode I crack. By using Griffith's plate complete linear elastic stress field, Sousa et al[17] improved estimates of plastic zone around crack tip. Camas et al[18] presented a novel methodology combining the strengths of both finite element modelling and image correlation. All these researches are mainly based on the Tresca, Mises, and the unified strength criteria; these criteria are available for the metal materials. However, it is well known that the above failure criteria is not suitable for rocks.[19-22] It is also well known that the Mohr-Coulomb criterion is considered to reasonably model the strength properties of isotropic rocks. Therefore, the Mohr-Coulomb criterion is introduced to derive the analytic solution of the plastic zone near crack tip in rocks in this paper.

Peridynamics, which is non-local, was introduced by Silling[23-25] in an attempt to deal with the discontinuities; it uses displacements rather than displacement derivatives in its formulation. Basically, the peridynamic theory is a reformation of the motion in solid mechanics that is well used to model bodies with cracks. The peridynamic theory uses spatial integral equations to analyse a discontinuity. This stands in contrast to the partial differential equations used in the classical formulation, which is not defined at discontinuities. The peridynamic governing equations are defined at fracture surfaces. Additionally, material damage is part of peridynamic constitutive laws. These attributions permit initiation and propagation of cracks to be modelled, with arbitrary parts, without the need for special crack growth treatment. This is because the model treats all forces between particles in a continuum as they act across a finite distance, in contrast with the fundamental assumption in the classical theory that all forces internal to a body result from contact. Peridynamic theory has been successfully applied to rock engineering. Rabczuk and Ren[26]presented a peridynamics formulation for quasi-static fracture and contact in rocks. Lee et al[27-29] obtained the crack coalescence morphology in rock-like material under compression using peridynamic theory. Peridynamic theory is divided into bond-based peridynamic theory and state-based peridynamic theory by Silling et al,[25] and state-based peridynamic theory is divided into ordinary state-based peridynamics and non-ordinary state-based peridynamics. When the force density vectors are parallel to the relative position vector and force density vectors of a bond has unequal magnitudes, it is called ordinary state-based

peridynamics. When the force density vectors are not parallel to the relative position vector, it is called non-ordinary state-based peridynamics. A non-local ordinary state-based plasticity model for peridynamics is put forward by Mitchell et al.[30] In ordinary state-based peridynamics, module state, which represents the linearization of an ordinary state-based constitutive model, is introduced. Ordinary state-based peridynamics can not only be used to model the propagation and coalescence process but also simulate the alternation of the radius of plastic zone at the crack tips. In this paper, the estimation of the plastic zone near the crack tips in rocks is done using the ordinary state-based peridynamics, and it is compared with the analytical solutions of plastic zone around crack tip in rocks under tensile loads.

The paper is organized as follows: In Section 2, the plasticity model of the ordinary state-based peridynamics is introduced. Analytical solutions of plastic zone near crack tips under tensile loading condition are obtained using Mohr-Coulomb criterion in Section 3. The comparisons between the numerical results and analytical solution are made; the numerical prediction of the plastic zone in the multiple cracks is done in Section 4. Conclusions are then drawn in Section 5.

2 THE PLASTIC MODEL OF ORDINARY STATE-BASED PERIDYNAMICS

2.1 The theory of the plastic model of ordinary state-based peridynamics

An ordinary state-based peridynamic theory is introduced; its basic equation is given as follows[25]:

$$\rho\ddot{\mathbf{u}}(\mathbf{x},t) = \int_{H_x}\{\underline{\mathbf{T}}[\mathbf{x},t]\langle\mathbf{x}'-\mathbf{x}\rangle - \underline{\mathbf{T}}[\mathbf{x}',t]\langle\mathbf{x}-\mathbf{x}'\rangle\}dV_{\mathbf{x}'} + \mathbf{b}(\mathbf{x},t) = \mathbf{L}(\mathbf{x},t) + \mathbf{b}(\mathbf{x},t) \quad (1)$$

The above equation is the peridynamics representation of Newton's second law for the Lagrangian point **x** and defines the internal force vector **L**(**x**, *t*). The function **b**(**x**, *t*) denotes a body force per unit volume. $\underline{\mathbf{T}}[\mathbf{x},t]\langle\mathbf{x}'-\mathbf{x}\rangle$ is a vector force state function and is somewhat analogous to stress tensor in local continuum mechanics in the sense that it represents the material response due to deformations. The force state function can be expressed as follows:

$$\underline{\mathbf{T}} = t\underline{\mathbf{M}} \quad (2)$$

where $\underline{t}$ is the scalar state of the force state and $\underline{\mathbf{M}}$ is the direction vector state of the force state.

A key gradient in the peridynamics constitutive model for plasticity is the decomposition of the scalar extension state into dilation and deviatoric parts, as well as the additive decomposition of deviatoric extension state into elastic part e^{de} and plastic parts e^{dp}, its expressions are written as follows:

$$e^d = e^{dp} + e^{de} \quad (3)$$

Therefore, the isotropic elastic constitutive model in a two dimension condition is written using the additive decomposition as follows[25]:

$$\underline{t} = \underline{t}^i + \underline{t}^d = \frac{2p}{m}\omega\underline{x} + \alpha\omega\left(e^d - e^{dp}\right) \quad (4)$$

where $\underline{t}^i$ is the co-isotropic part of $\underline{t}$ and $\underline{t}^d$ is the co-deviatoric part of $\underline{t}$, $p = -k\theta$ is the peridynamic pressure, k is the bulk modulus, θ is the volumetric strain, $\underline{x}$ is the reference position scalar state field, m is the weighted volume, and ω is the influence function.

A rate form of the above equation in two dimension is given as follows:

$$\dot{t} = \dot{t}^i + \dot{t}^d = \frac{2k\dot{\theta}}{m}\omega\underline{x} + \alpha\omega\left(\dot{e}^d - \dot{e}^{dp}\right) \quad (5)$$

where $\dot{\theta} = \theta(\dot{e})$, the above relations follow from the fact that there exists an elastic stored energy functional W as the following form[25];

$$W\left(\theta, e^d, e^{dp}\right) = \frac{k\theta^2}{2} + \frac{\alpha}{2}\omega\left(e^d - e^{dp}\right)\cdot\left(e^d - e^{dp}\right) \quad (6)$$

The strategy is to define a yield surface in S_d, the space of co-deviatoric force states:

$$S_d = \left\{t^d \in S \middle| t^d \cdot x = 0\right\} \quad (7)$$

where S_d is a subspace of S.

To use the elastic constitutive relation for plasticity calculation, a scalar valued function f, which is called the yield function, is used to define a set of allowable scalar deviatoric force states $\underline{E}$ as follows:

$$\underline{E} = \left\{t^d \in S^d \middle| f\left(t^d\right) = \psi\left(t^d\right) - \psi_0 \leq 0\right\} \quad (8)$$

where ψ_0 is a positive constant, which represents the yield point of the material, ψ is a function on f and S_d.

Note that *f* does not include hardening. This form of *f* is analogous to local perfect plasticity. The plastic flow rule is defined as follows:

$$e^{dp} = \lambda \nabla^d \psi \quad (9)$$

where $\nabla^d \psi$ is Frechet derivative[25] of $\psi \in S$ on S_d, λ is the so-called consistency parameter, the key idea is that $\nabla^d \psi$ produces functions that have no dilation. Given $\{e^d_{n+1}, e^d_n, e^{dp}_n\}$, the problem is to find e^{dp}_{n+1}; this approach to integration is extension state driven and is analogous to the strain-driven approach used in local plasticity.

At step *n*, corresponding to time t_n, the scalar deviatoric extension state e^d_n and the deviatoric plastic extension state e^{dp}_n are denoted as follows:

$$e^d_n = e^d(t_n), e^{dp}_n = e^{dp}(t_n) \quad (10)$$

Using the flow rule given in Equation 9 and the constitutive model for t_d, a trial value for the deviatoric force state t^d_{trial} is defined and computed as follows[30]:

$$\begin{aligned} t^d_{n+1} &= \alpha \underline{\omega}\left(e^d_{n+1} - e^{dp}_{n+1}\right) = \alpha \underline{\omega}\left(e^d_{n+1} - e^{dp}_n\right) - \alpha \underline{\omega}\left(e^{dp}_{n+1} - e^{dp}_n\right) \\ &= t^d_{trial} - \alpha \underline{\omega} \Delta\lambda \nabla^d \psi \end{aligned} \quad (11)$$

where $\Delta\lambda = \lambda \Delta t$.
Given t^d_{trial}, the yield function $f\left(t^d_{trial}\right)$ is used to determine if the step is elastic or incrementally plastic.

If $f\left(t^d_{trial}\right) < 0$, then the loading/unloading conditions are automatically satisfied with $\Delta\lambda = 0$, this leads to the following:

$$t^d_{n+1} = t^d_{trial} \quad (12)$$

$$e^{dp}_{n+1} = e^{dp}_n \quad (13)$$

If $f\left(t^d_{trial}\right) > 0$, then the step is incrementally plastic and $\Delta\lambda > 0$. In this case, for the yield function *f* defined by $\psi\left(t^d\right) = \frac{\|t_d\|^2}{2}$ and $\omega = 1$, and using Equation 11, the deviatoric force state at the end of the step is obtained as follows:

$$t^d_{n+1} = \frac{t^d_{trial}}{1 + \alpha\Delta} \lambda \quad (14)$$

Therefore, the value of the yield function at the end of the step is given by the following:

$$f(t_{n+1}^d) = \frac{\|t_{trial}^d\|^2}{2} \frac{1}{(1+\alpha\Delta\lambda)^2} - \psi_0 \quad (15)$$

Setting the above equal to zero yields a value for $\Delta\lambda$ as follows:

$$\Delta\lambda = \frac{1}{\alpha}\left(\frac{\|t_{trial}^d\|}{\sqrt{2\psi_0}} - 1\right) \quad (16)$$

The deviatoric force and plastic states are updated as follows:

$$t_{n+1}^d = \sqrt{2\psi_0}\frac{t_{trial}^d}{\|t_{trial}^d\|}, e_{n+1}^{dp} = e_n^{dp} + \frac{1}{\alpha}\left(\frac{\|t_{trial}^d\|}{\sqrt{2\psi_0}} - 1\right) t_{n+1}^d \quad (17)$$

The approach is corresponding to a state of pure shear at a point. This will be induced by a prescribed infinitesimal displacement field. A displacement field induced by pure shear is given by the following:

$$u(\xi) = \gamma b\hat{i} \quad (18)$$

where γ is shear strain and $\hat{i}$ denotes the coordinate axis unit vector in the a direction. A point in the undeformed configuration in two dimension is located by the triplet (a, b) which is relative to the centre of a circle. Ultimately, integral will be done on a sphere of radius δ.

The scalar deformation state is written as a function[30] of γ:

$$Y(\gamma) = \sqrt{b^2 + (a+b\gamma)^2} \quad (19)$$

The scalar extension state becomes as follows:

$$e = |Y| - |\xi| = |\xi|\gamma \sin\theta\cos\theta \quad (20)$$

Note that (ξ, θ) are spherical coordinates. θ should not be considered as the dilation; using the above scalar extension state, it can be shown that the dilation is zero. Furthermore, since the dilation is zero, the scalar extension state and deviatoric extension state are identical.

To evaluate the yield condition within ordinary state-based peridynamics, the quantity $\|e^d\|^2$must be evaluated. This is given by integrating over a circle of radius δ, this value is expressed as follows:

$$\|e^d\|^2 = \frac{\pi\gamma^2\delta^4}{16} \quad (21)$$

Given the deviatoric extension state e^d in Equation 21, the associated scalar force state is deviatoric and is given by the following:

$$t^d = \alpha e^d = \frac{8\mu}{m}|\xi|\gamma \sin\theta\cos\theta \quad (22)$$

This value is substituted into the yield functional; the following expression is obtained as follows:

$$\psi_0 = \frac{\|t_d\|^2}{2} = \frac{1}{2}\left(\frac{8\mu}{m}\right)^2 \|e^d\|^2 = \frac{8\left(\mu\gamma_y\right)^2}{\pi \quad \delta^4} = \frac{8E^2}{\pi\delta^4} \quad (23)$$

where γ_y denotes shear strain at material yield and a value of $m = \frac{\pi\delta^4}{2}$ was used for the weighted volume.

A yield stress corresponding to a state of pure shear is identified and defined as follows:

$$E_y = \mu\gamma_y \quad (24)$$

To understand the value of E_y under conditions of uniaxial tension, effective stress σ_e is considered; the effective stress is expressed using the second invariant J_2 but can be written in terms of the stress tensor components σ_{ij} and its principle values $\{\sigma_1, \sigma_2, \sigma_3\}$, then σ_e can be expressed as follows:

$$\begin{aligned}\sigma_e^2 = 3J_2 &= \frac{1}{6}\left[(\sigma_{11}-\sigma_{22})^2 + (\sigma_{22}-\sigma_{33})^2 + (\sigma_{33}-\sigma_{11})^2\right] \\ &\quad \times + \sigma_{12}^2 + \sigma_{32}^2 + \sigma_{13}^2, \\ &= \frac{1}{6}\left[(\sigma_1-\sigma_2)^2 + (\sigma_2-\sigma_3)^2 + (\sigma_3-\sigma_1)^2\right]\end{aligned} \quad (25)$$

The yield function is $f(\sigma_e, E_y) = 0$, then it is written as follows:

$$f\left(\sigma_e, E_y\right) = \sigma_e - E_y = 0 \quad (26)$$

When yield stress is measured under uniaxial stress, $\sigma_1 \neq 0$, $\sigma_2 = \sigma_3 = 0$, namely,

$$f\left(\sigma_e, E_y\right) = \frac{\sigma_1}{\sqrt{3}} - E_y = 0 \Rightarrow E_y = \frac{\sigma_1}{\sqrt{3}} \quad (27)$$

2.2 Discretization and numerical implementation

In discrete system, each material point contains the deformation information. The velocities and displacements for each peridynamic material point $\mathbf{x}_i$ in the media are, respectively, given by the following:

$$\dot{\mathbf{u}}(\mathbf{x}_i, t+\Delta t) = \dot{\mathbf{u}}(\mathbf{x}_i, t) + \ddot{\mathbf{u}}(\mathbf{x}_i, t)\Delta t \quad (28)$$

$$\mathbf{u}(\mathbf{x}_i, t+\Delta t) = \mathbf{u}(\mathbf{x}_i, t) + \dot{\mathbf{u}}(\mathbf{x}_i, t)\Delta t \quad (29)$$

Then the integration in Equation 1 can be expressed using Riemann sums over the total number of particles within the horizon H_x. Therefore, the plastic model of the ordinary state-based peridynamic governing equation for the given PD particle can be approximated as follows:

$$\rho \frac{\mathbf{u}(\mathbf{x}_i, t+\Delta t) - 2\mathbf{u}(\mathbf{x}_i, t) + \mathbf{u}(\mathbf{x}_i, t-\Delta t)}{\Delta} t^2 = \sum_{n=1}^{m} \{\underline{\mathbf{T}}[\mathbf{x}_n, t]\langle \mathbf{x}_n - \mathbf{x}_i \rangle - \underline{\mathbf{T}}[\mathbf{x}_i, t]\langle \mathbf{x}_i - \mathbf{x} \quad (30)$$

Damage of a peridynamic material particle $\mathbf{x}_i$ can be locally given in terms of the ratio of amount of broken bonds to the total amount of interaction in one horizon as

$$D(\mathbf{x}_i, t) = 1 - \frac{\int_{H_x} \mu(\mathbf{x}_i, t) dV_{\mathbf{x}_j}}{\int_{H_x} dV_{\mathbf{x}_j}}. \quad (31)$$

where $\mu(\mathbf{x}_i, t)$ is a scalar factor representing the broken of bond

$$\mu(\mathbf{x}_i, t) = \begin{cases} 1 & \text{unbroken} \\ 0 & \text{broken} \end{cases}. \quad (32)$$

3 ANALYTICAL SOLUTION OF PLASTIC ZONE NEAR CRACK TIPS UNDER TENSILE LOADS

Estimation of the plastic zone near crack tips under small-scale yielding (SSY) is one of the important topics in elastic-plastic fracture mechanics. It is known as Irwin's plastic zone correction model; the shape and size of yielding zone were derived from the Huber-von Mises criterion. Irwin31 further extended his model for plane-strain condition by enhancing the yield stress by a factor of $\sqrt{3}$. Broke32 presented his estimation using the Tresca criterion. The above-mentioned models are all based on the SSY condition and are constructed with the assumptions in the linear elastic fracture mechanics. They yield reasonably good estimations for certain materials such as metals having equal tensile and compressive strength. However, these criteria will not be suitable for the rock-like materials; if the material of rock and soil is regarded as an ideal plasticity,

Mohr-Coulomb criterion is fit to estimate the plastic zone near crack tips under SSY. The Mohr-Coulomb criterion is expressed as follows:

$$F = \frac{1}{2}(\sigma_1 - \sigma_3) + \frac{1}{2}(\sigma_1 + \sigma_3)\sin\phi - c\cos\phi, \quad (33)$$

where σ_1 and σ_3 is, respectively, the maximum and minimum principle stress, c is cohesive force, and ϕ is internal friction angle.

By virtue of linear elastic fracture mechanics, the 2D stress field in the vicinity of the mode I crack tip can be described as follows[33]:

$$\begin{Bmatrix} \sigma_x \\ \sigma_y \\ \tau_{xy} \end{Bmatrix} = \frac{K_I}{\sqrt{2\pi r}}\cos\frac{\theta}{2}\begin{Bmatrix} 1 - \sin(\theta/2)\sin(3\theta/2) \\ 1 + \sin(\theta/2)\sin(3\theta/2) \\ \sin(\theta/2)\cos(3\theta/2) \end{Bmatrix}, \quad (34)$$

where K_I is stress intensity factor for mode I cracks; σ_x,σ_y are the normal stresses in x- and y-direction, respectively; and τ_{xy} is the shear stress in the xy-direction. Position vector is expressed in polar coordinate (r, θ) measured from the crack tip.

The stress components in Equation 34 can be expressed in terms of the principal stresses σ_i.

For two-dimensional plane problem, the principal stresses are obtained as follows:

$$\begin{Bmatrix} \sigma_1 \\ \sigma_3 \end{Bmatrix} = \frac{\sigma_x + \sigma_y}{2} \pm \sqrt{\left(\frac{\sigma_x - \sigma_y}{2}\right)^2 + \tau_{xy}^2}, \quad (35)$$

$$\sigma_2 = \begin{cases} 0 & \text{plane stress} \\ \nu(\sigma_1 + \sigma_2) & \text{plane strain} \end{cases}, \quad (36)$$

in which ν is Poisson's ratio.

It is assumed that $\sigma_1 \geq \sigma_2 \geq \sigma_3$, by substituting Equation 34 into Equations 35 and 36, the resulting stresses are obtained as follows:

a. Under plane stress condition, the following expression is written:

$$\begin{Bmatrix} \sigma_1 \\ \sigma_3 \end{Bmatrix} = \frac{K_I}{\sqrt{2\pi r}}\cos\frac{\theta}{2}\left(1 \pm \sin\frac{\theta}{2}\right), \quad (37a)$$

$$\sigma_2 = 0. \quad (37b)$$

2. Under plane strain condition, the following expression is obtained:

$$\left.\begin{matrix}\sigma_1\\ \sigma_3\end{matrix}\right\} = \frac{K_I}{\sqrt{2\pi r}}\cos\frac{\theta}{2}\left(1 \pm \sin\frac{\theta}{2}.\right) \quad \text{for} \quad 0 \le \theta \le 2\sin^{-1}(1-2\nu),$$
$$\sigma_2 = \frac{2\nu K_I}{\sqrt{2\pi r}}\cos\frac{\theta}{2}. \tag{38}$$

For plane stress condition, substituting Equation 37 into Equation 33, the formulate of shape and size of plastic zone near mode I crack tips can be obtained as follows:

$$r_p = \frac{K_I^2}{8\pi c^2\cos^2\phi}\cos^2\frac{\theta}{2}\left(1 + \sin\frac{\theta}{2}\right)^2(1 + \sin\phi)^2. \tag{39}$$

For plane strain condition, substituting Equation 38 into Equation 33, the formulate of shape and size of plastic zone near mode I crack tips can be expressed as follows:

$$r_p = \frac{K_I^2}{2\pi c^2\cos^2\phi}\cos^2\frac{\theta}{2}\left[\frac{1}{2}\left(1 + \sin\frac{\theta}{2}\right)(1 + \sin\phi) - \nu(1 - \sin\phi)\right]^2. \tag{40}$$

4 COMPARISON BETWEEN PERIDYNAMIC SOLUTION AND ANALYTICAL SOLUTION OF PLASTIC ZONE AROUND CRACK TIPS

4.1 Prediction of plastic zone around a horizontal crack tips subjected to uniaxial tension

There is a rectangular rock sample with the length of 0.10 m and width of 0.05 m. The rectangular rock sample is divided into 200 × 100 = 20 000 discrete nodes. The grid space between adjacent two points is $\Delta x = 5 \times 10^{-4}$ m. The calculation parameters are listed as follows: $\delta = 3\Delta x$, $s_0 = 0.082$, Young's modulus is E = 100 GPa, the mass density ρ is 2200 kg/m^3, Poisson's ratio ν is 0.30, c = 6 MPa, and $\phi = 40^o$. Based on the previous studies in peridynamics,[34] the horizon size $\delta = 3\Delta x$ is recommended to study mechanical behaviours of cracks. Moreover, as stated by Cheng et al,[35] when the ratio of $\delta/\Delta x$ is larger than 3 times, the horizon size has no significant influence on cracking behaviours. Thus, in this study, the ratio of $\delta/\Delta x$ is taken as three. Because dynamic analysis is used, the recommended time step 5.33×10^{-8} seconds is specified. Its geometric configuration is plotted in Figure 1. When time step arrives at 450, radius of plastic zone near the crack tip is plotted in Figure 2.

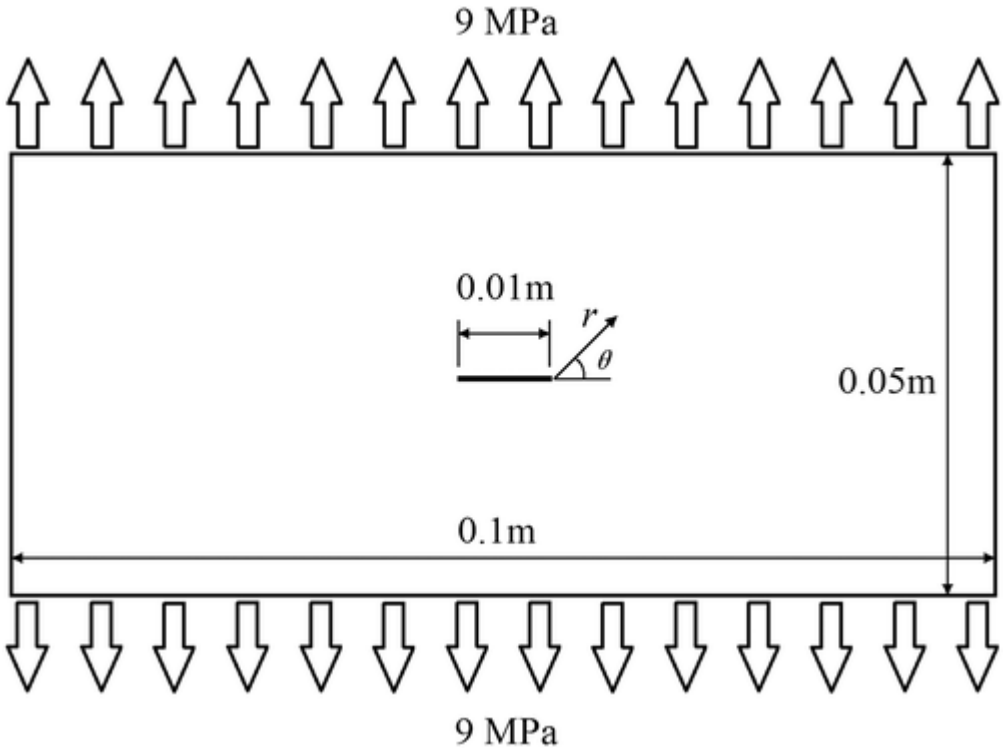

Figure 1

Open in figure viewerPowerPoint

The geometric configuration

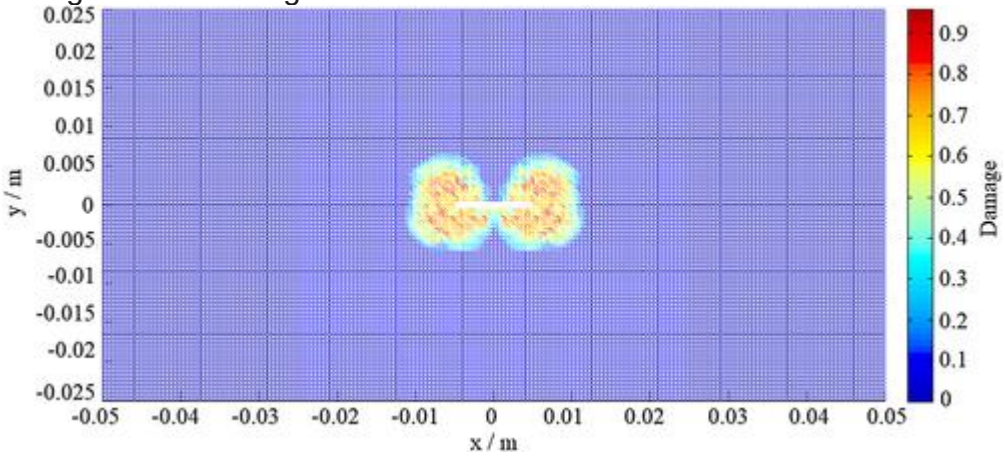

Figure 2

Open in figure viewerPowerPoint

The numerical results of the plastic zone near the crack tips obtained from peridynamics [Colour figure can be viewed at wileyonlinelibrary.com]

Comparison of the plastic zone radius obtained from peridynamic and analytic solution is plotted in Figure 3. It can be observed from Figure 3 that the relative error between peridynamic solution and the analytical solution is very little. For example, the relative error is 1.82% when $\theta = 30^{\circ}$; the relative error is 2.47% when $\theta = 120^{\circ}$. Therefore, the radius of the plastic zone obtained from peridynamic solution is in good agreement with

that obtained from the analytical solution. It is feasible to evaluate the plastic zone radius around crack tips by using peridynamics.

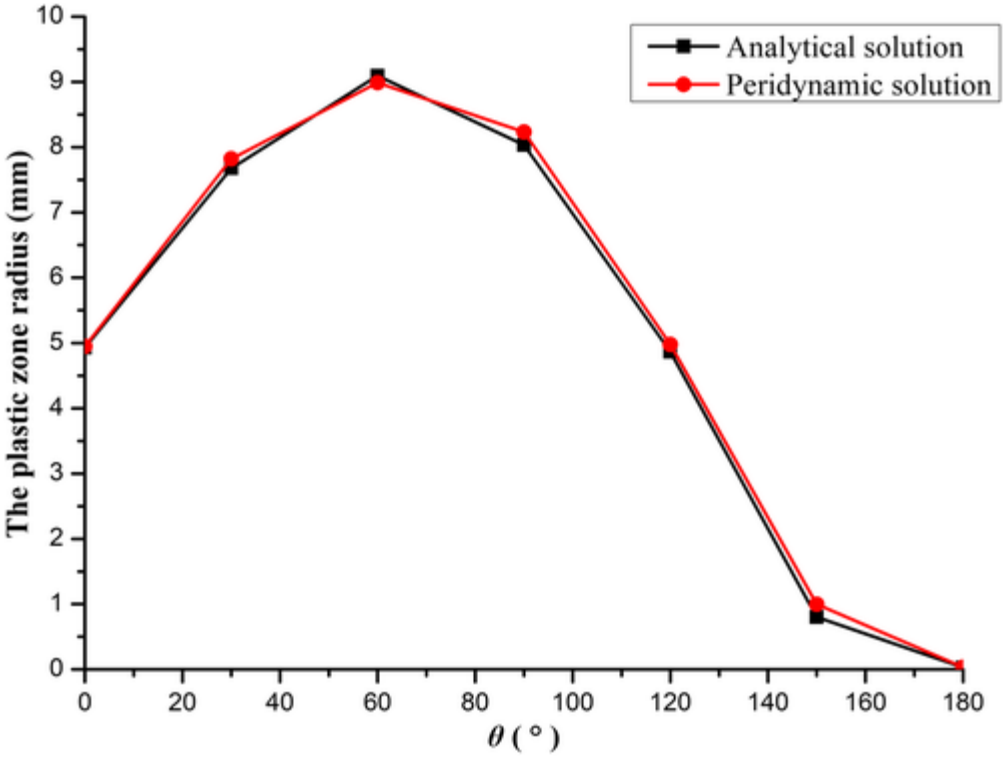

Figure 3
Open in figure viewerPowerPoint
Comparison of the plastic zone radius obtained from peridynamic and analytical solutions [Colour figure can be viewed at wileyonlinelibrary.com]

4.2 Prediction of plastic zone around crack tips with the inclination angle of 45°

There is a rectangular rock sample with the length of 0.10 m and width of 0.05 m. The rectangular rock sample is divided into 200 × 100 = 20 000 discrete nodes. The grid space between adjacent two points is $\Delta x = 5 \times 10^{-4}$ m. The calculation parameters are listed as follows: $\delta = 3\Delta x$, $s_0 = 0.082$, Young's modulus is E = 100GPa, the mass density ρ is 2200 kg/m^3, Poisson's ratio v is 0.30, c = 6 MPa, and $\phi = 40^\circ$. Because dynamic analysis is used, the recommended time step 5.33×10^{-8} seconds is specified. Its geometric configuration is plotted in Figure 4. When time step arrives at 450, plastic zone radius near the crack tips is plotted in Figure 5.

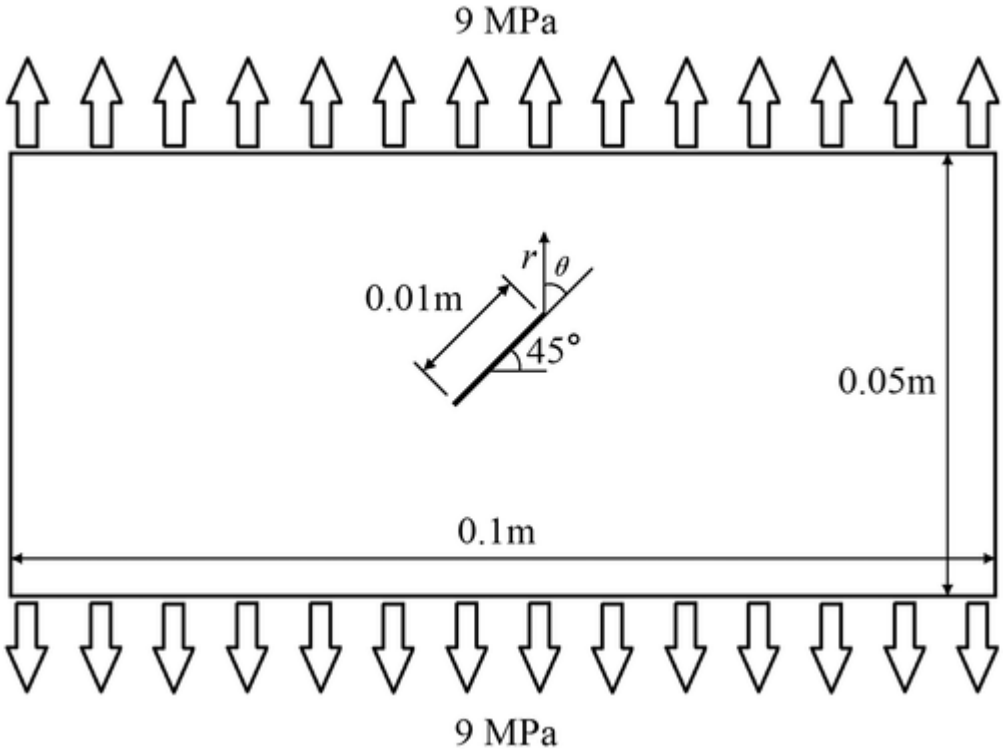

Figure 4

Open in figure viewerPowerPoint

The geometric configure of the crack with the inclination angle of 45°

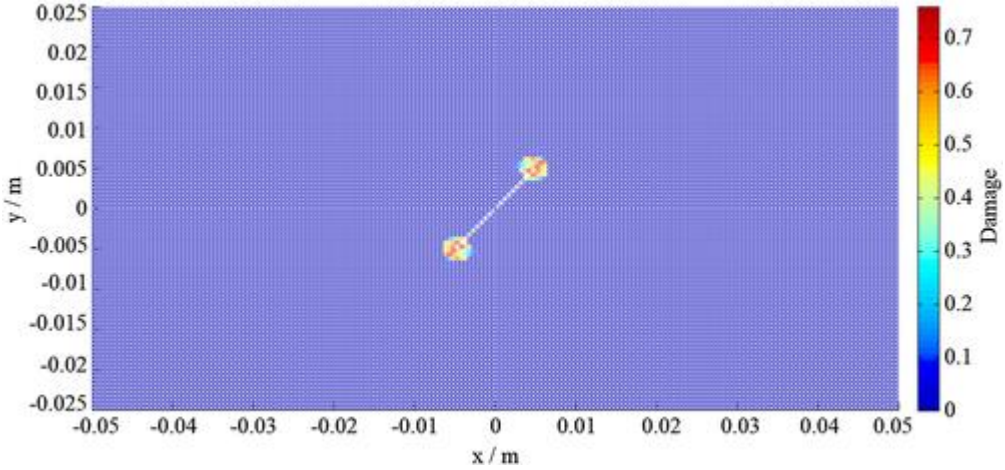

Figure 5

Open in figure viewerPowerPoint

Peridynamic simulation of plastic zone around crack tips with the inclination angle of 45°[Colour figure can be viewed at wileyonlinelibrary.com]

Comparison of the plastic zone radius obtained from peridynamic and analytic solution is plotted in Figure 6. It can be found from Figure 6 that the relative error between the analytical and peridynamic solution is very little. For example, the relative error is −3.64% when $\theta = 30^{\circ}$; the relative error is −2.46% when $\theta = 120^{\circ}$. Therefore, the value

of the radius of the plastic zone obtained from peridynamic solution is in good agreement with that obtained from the analytical solution.

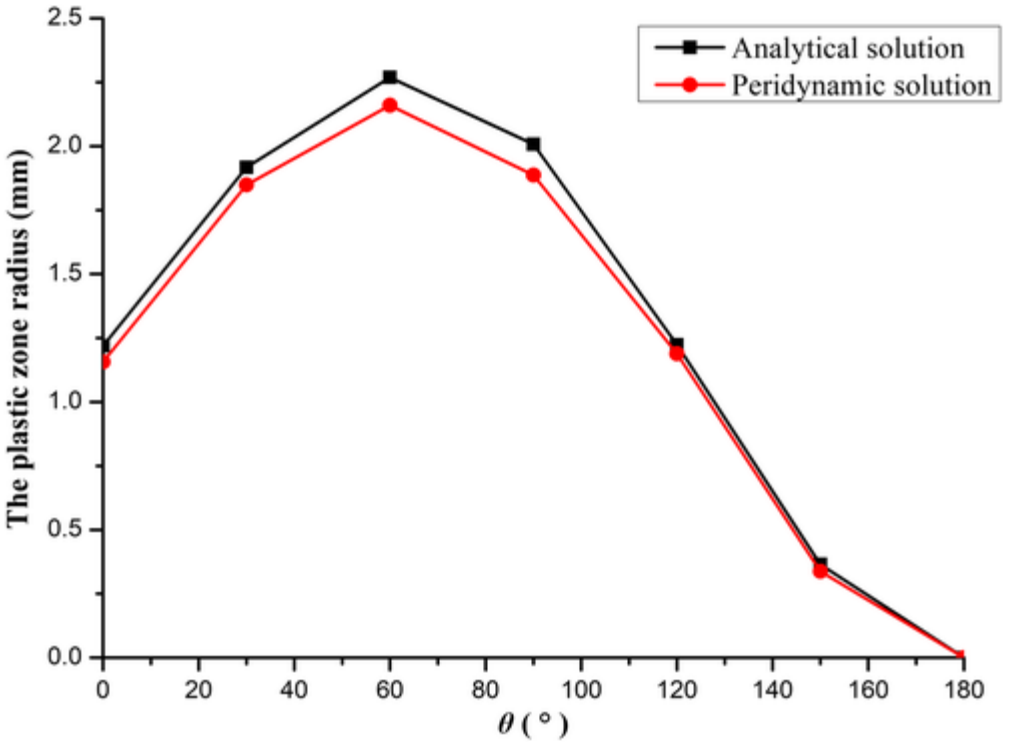

Figure 6
Open in figure viewerPowerPoint
Comparison of plastic zone radius near crack tips with the inclination angle of 45° obtained from peridynamic and analytic solutions [Colour figure can be viewed at wileyonlinelibrary.com]

4.3 Prediction of plastic zone around crack tips with the inclination angle of 30°

The physical and geometric parameters are the same as the above examples. Because dynamic analysis is used, the recommended time step 5.33×10^{-8} seconds is specified. Its geometric configuration is plotted in Figure 7. When time step arrives at 400, the plastic zone radius near the crack tips is plotted in Figure 8.

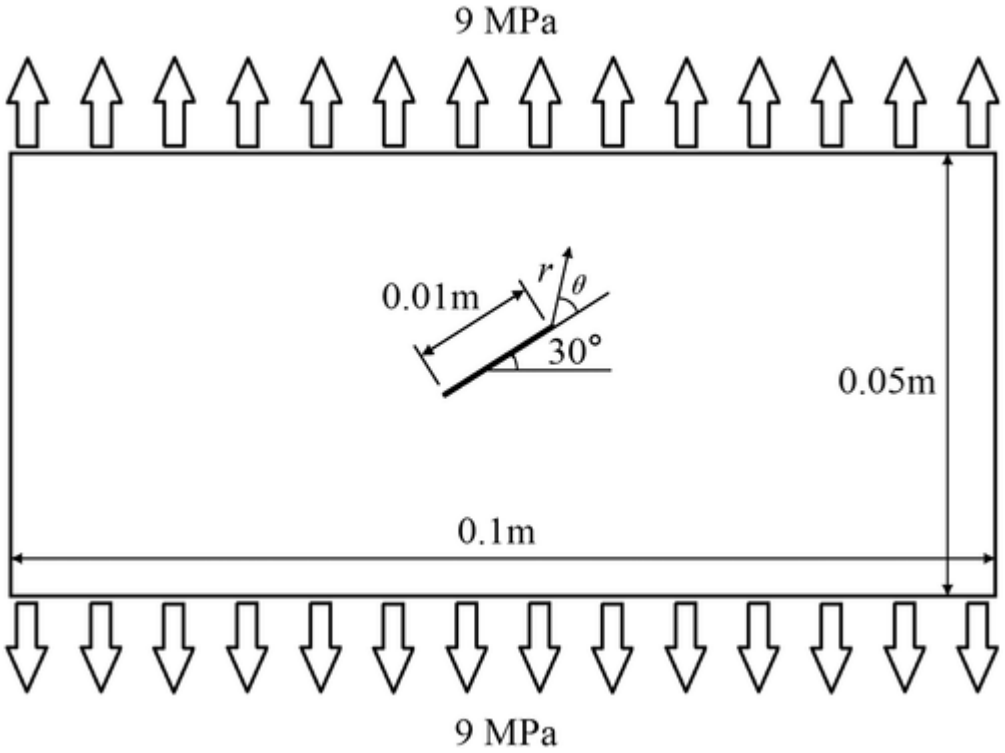

Figure 7

Open in figure viewerPowerPoint

The geometric configure of the crack with the inclination angle of 30°

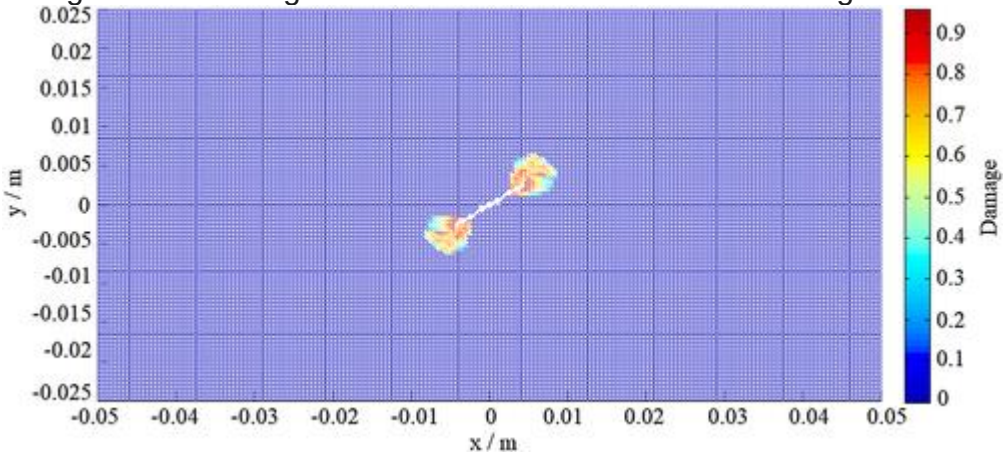

Figure 8

Open in figure viewerPowerPoint

Peridynamic simulation of plastic zone around crack tips with the inclination angle of 30°[Colour figure can be viewed at wileyonlinelibrary.com]

Comparison of the plastic zone radius obtained from peridynamic and analytical solution is plotted in Figure 9. It can be found from Figure 9 that the relative error between the analytical and peridynamic solution is very little. For example, the relative error is −2.70% when $\theta = 30^{\circ}$; the relative error is 1.11% when $\theta = 120^{\circ}$. Therefore, the value of

the radius of the plastic zone from peridynamic solution is in good agreement with that from the analytical solution.

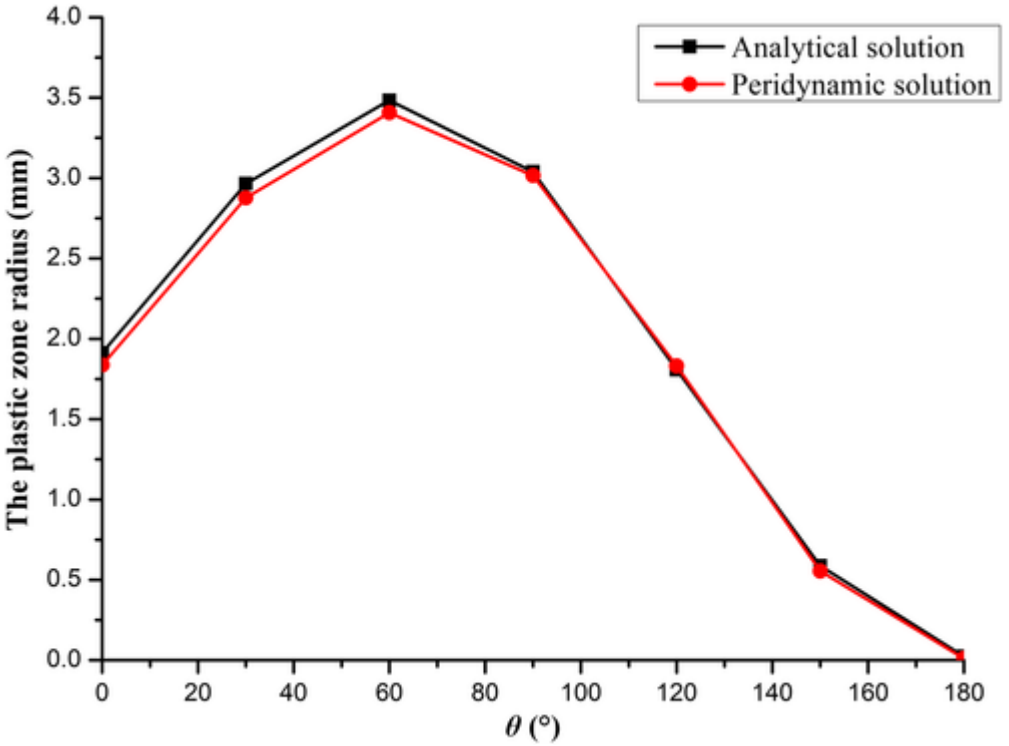

Figure 9
Open in figure viewerPowerPoint
Comparison of plastic zone radius near the crack tips with the inclination angle of 30°obtained from peridynamic and analytical solutions [Colour figure can be viewed at wileyonlinelibrary.com]

4.4 Prediction of plastic zones around two parallel crack tips with the inclination angle of 45°

The physical and geometric parameters are the same as the above example. Because dynamic analysis is used, the recommended time step 5.33×10^{-8} seconds is specified. Its geometric configuration is plotted in Figure 10. When time step arrives at 400, plastic zone radius near the crack tips is plotted in Figure 11. Comparison of the plastic zone radius around the inner tips of two parallel cracks and one crack is plotted in Figure 12.

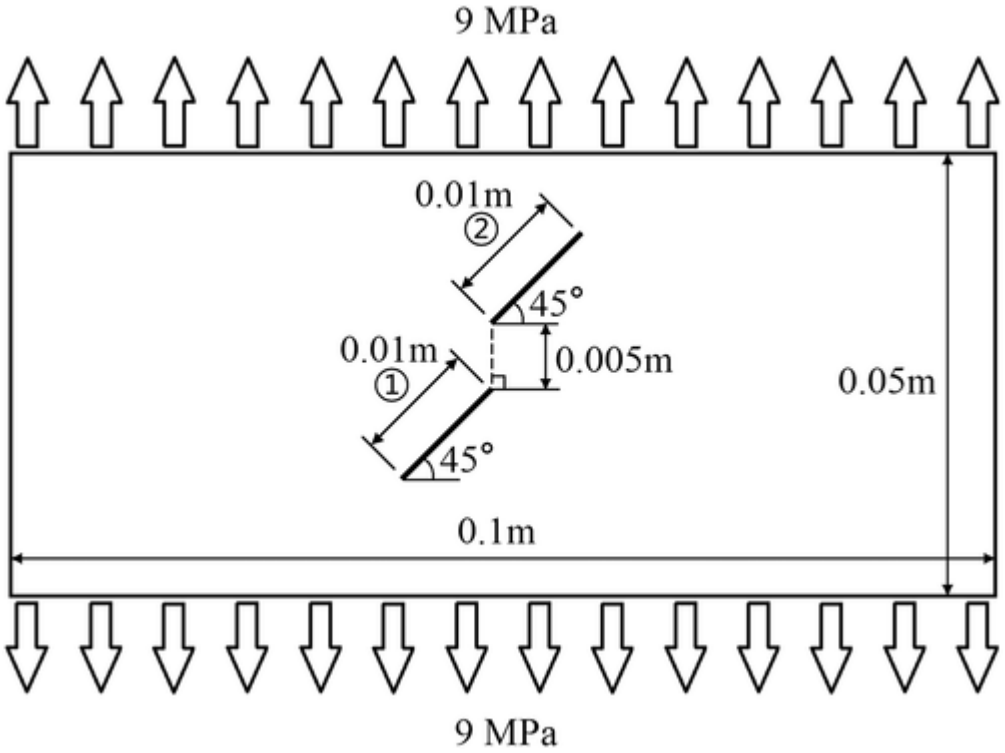

Figure 10

Open in figure viewerPowerPoint

The geometric configure of two parallel cracks with the inclination angle of 45°

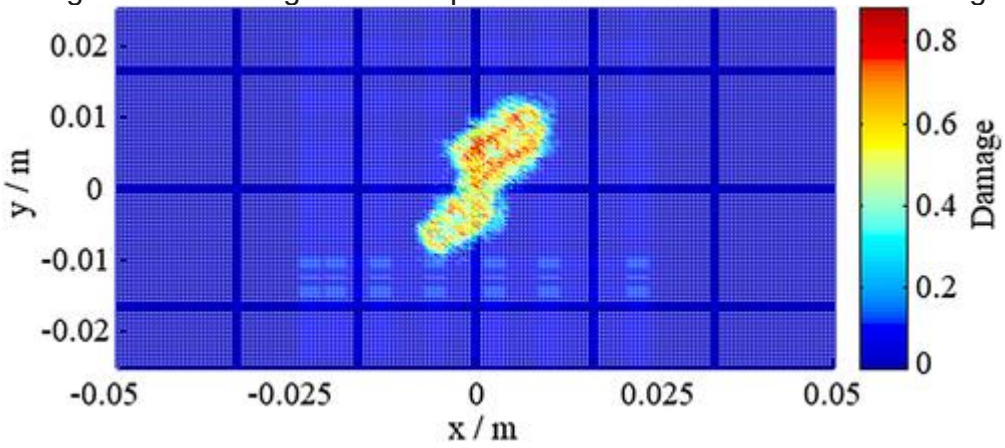

Figure 11

Open in figure viewerPowerPoint

Peridynamic simulation of plastic zone near the tips of two parallel cracks with the inclination angle of 45° [Colour figure can be viewed at wileyonlinelibrary.com]

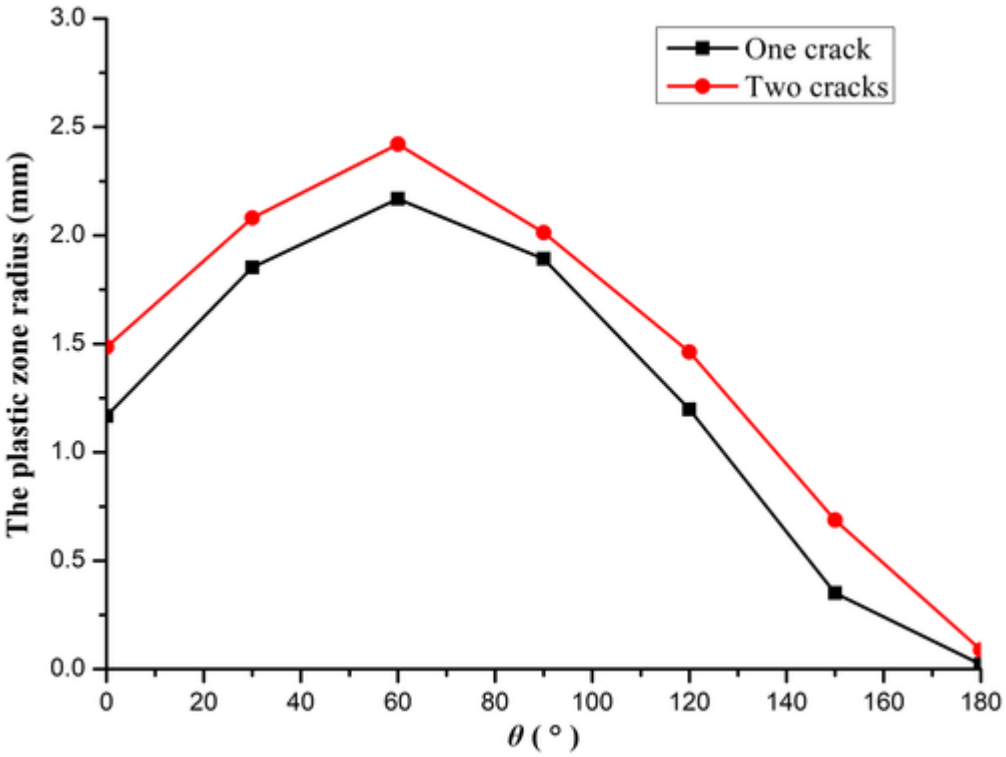

Figure 12
Open in figure viewerPowerPoint
Comparison of the plastic zone radius near the inner tips of two parallel cracks and the tips of single crack [Colour figure can be viewed at wileyonlinelibrary.com]

Peridynamic simulation of plastic zone is plotted in Figure 11. It can be observed from Figure 12 that the plastic zone radius near the inner tip of two parallel cracks is bigger than that near the tip of one crack. The main reason is that the interaction of the cracks leads to the strong amplification effects. It can also be found from Figure 11 that coalescence of the plastic zones near the crack tips occurs under uniaxial tension. Comparing the plastic zone radius near the outer tip of two parallel cracks and the tip of single crack, it can be seen from Figure 13 that the plastic zone radius near the tip of single crack is approximately equal to that around the outer tip of two parallel cracks.

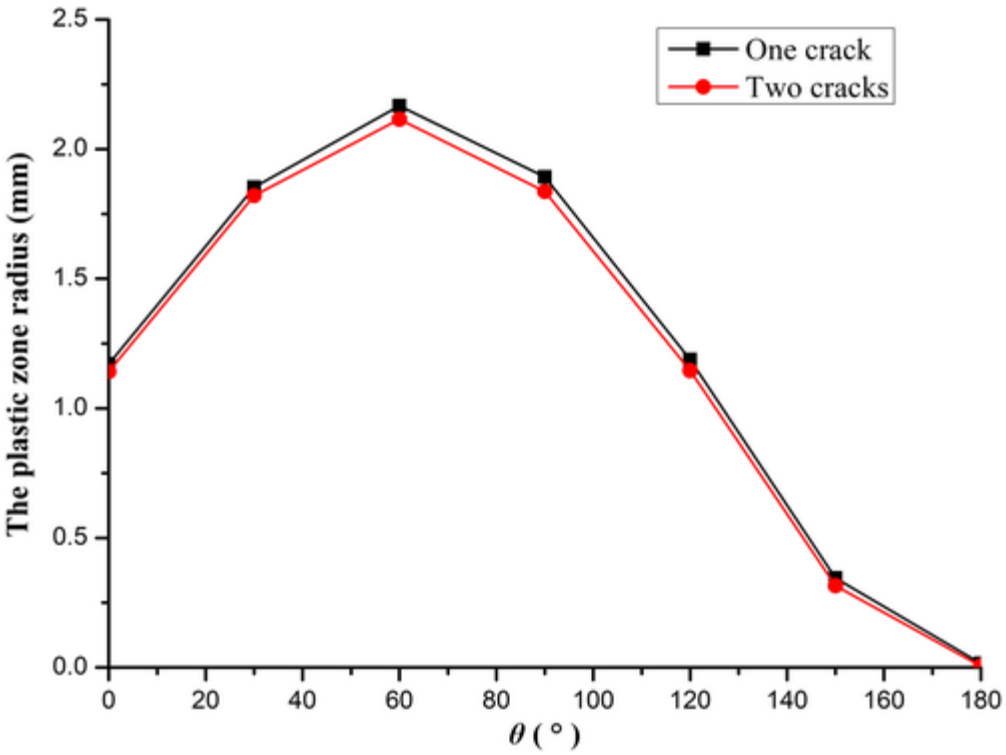

Figure 13
Open in figure viewerPowerPoint
Comparison of the plastic zone radius near the outer tips of two parallel cracks and the tips of single crack [Colour figure can be viewed at wileyonlinelibrary.com]

4.5 Prediction of plastic zones near 3 parallel crack tips with the inclination angle of 135°

The physical and geometric parameters are the same as the former section 4.2. There are 3 parallel cracks with the angle of inclination of 135° in the sample; the length of the cracks is 0.01 m, and the horizontal spacing between the cracks is 0.005 m. Its geometric configuration is plotted in Figure 14. The recommended time step is 5.33×10^{-8} seconds. When time step arrives at 220, plastic zones around the crack tips are plotted in Figure 15. Comparison of the plastic zone radius near the inner tip of 2 parallel cracks, 3 parallel cracks, and single crack with the inclination angle 135° is plotted in Figure 15.

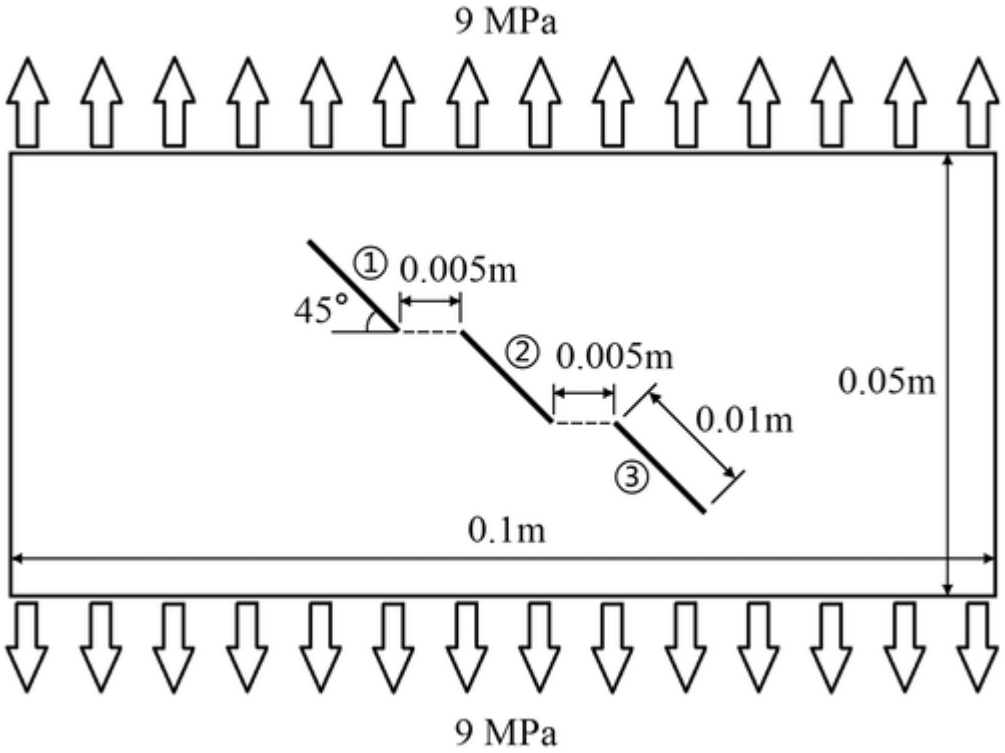

Figure 14

Open in figure viewerPowerPoint

The geometric configure with 3 parallel cracks

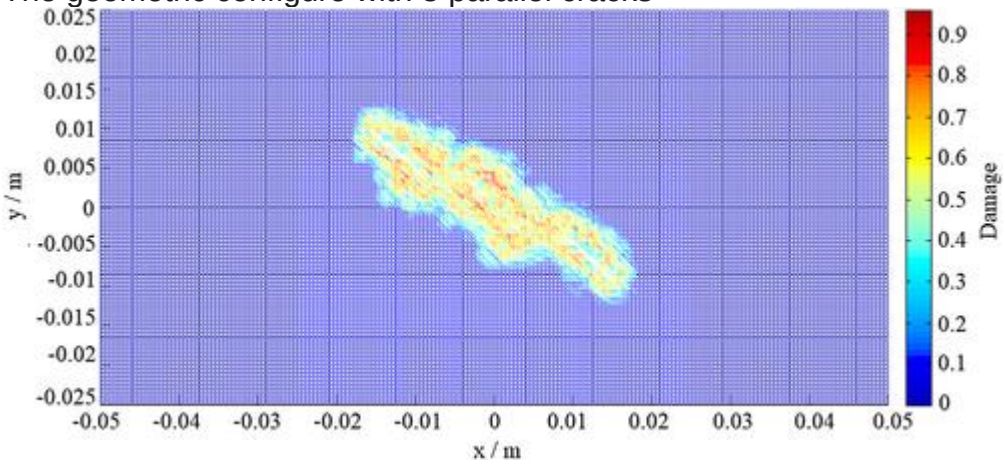

Figure 15

Open in figure viewerPowerPoint

Peridynamic simulation of plastic zone radius near the tips of 3 parallel cracks with the inclination angle of 135° [Colour figure can be viewed at wileyonlinelibrary.com]

Peridynamic simulation of plastic zone around the tips of 3 parallel cracks is plotted in Figure 15. It can be observed from Figure 16 that the plastic zone radius near the outer tip of crack ① in array of 3 parallel cracks is approximately equal to that in array of two parallel cracks and single crack. It is also found from Figure 17 that the plastic zone radius near inner tip of crack ① in array of 3 parallel cracks is the biggest and the

plastic zone radius near the tip of single crack is the smallest. Moreover, it can be seen from Figure 18 that the plastic zone radius near inner tip of crack ② in array of 3 parallel cracks is the biggest and the plastic zone radius near outer tip of crack ① in array of 3 parallel cracks are the smallest. The main reason is that the interaction of the cracks leads to the strong amplification effects.

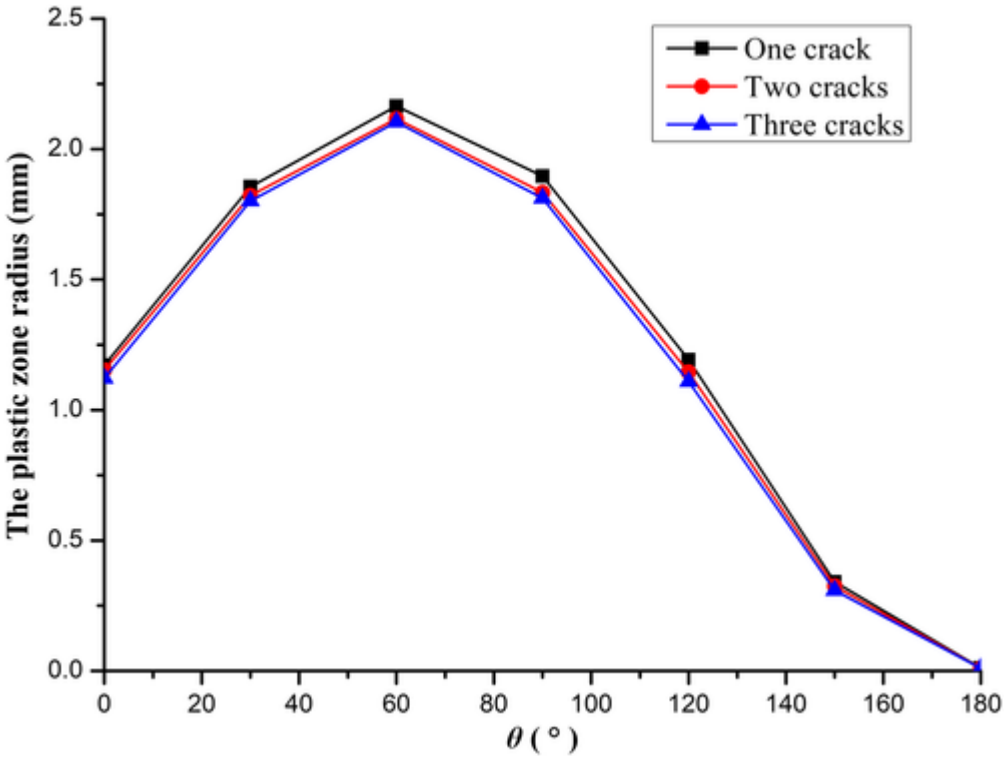

Figure 16
Open in figure viewerPowerPoint
Comparison of the plastic zone radius near the outer tip of 2 parallel cracks, 3 parallel cracks, and single crack with the inclination angle of 135° [Colour figure can be viewed at wileyonlinelibrary.com]

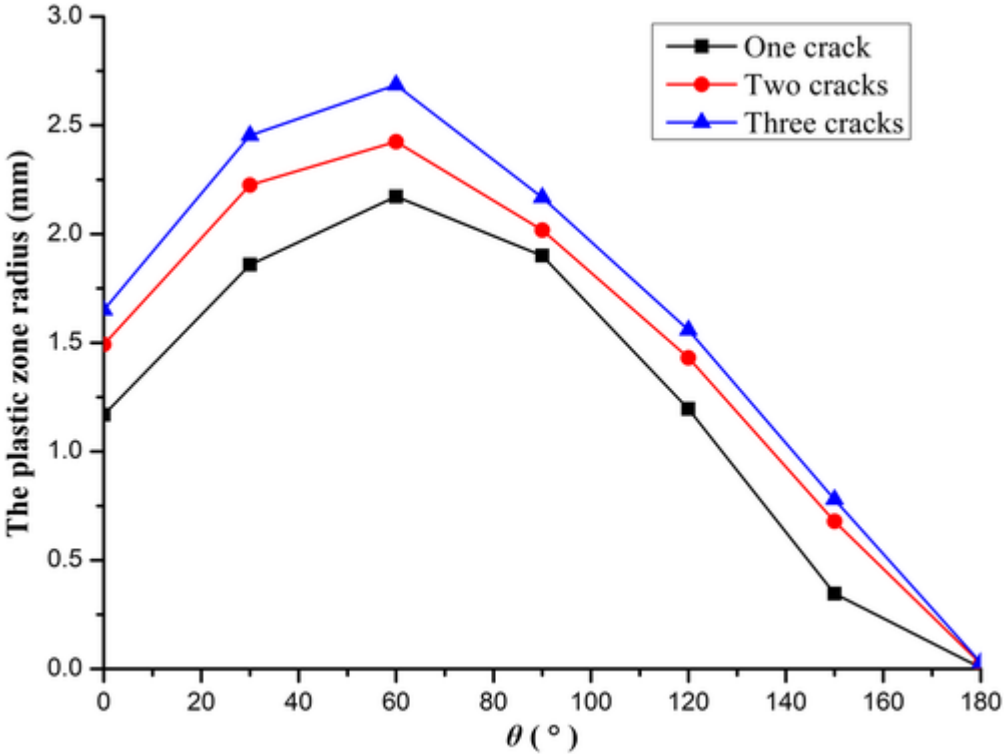

Figure 17

Open in figure viewerPowerPoint

Comparison of the plastic zone radius near the inner tip of the crack ① in array of 2 and 3 parallel cracks and single crack with the inclination angle of 135° [Colour figure can be viewed at wileyonlinelibrary.com]

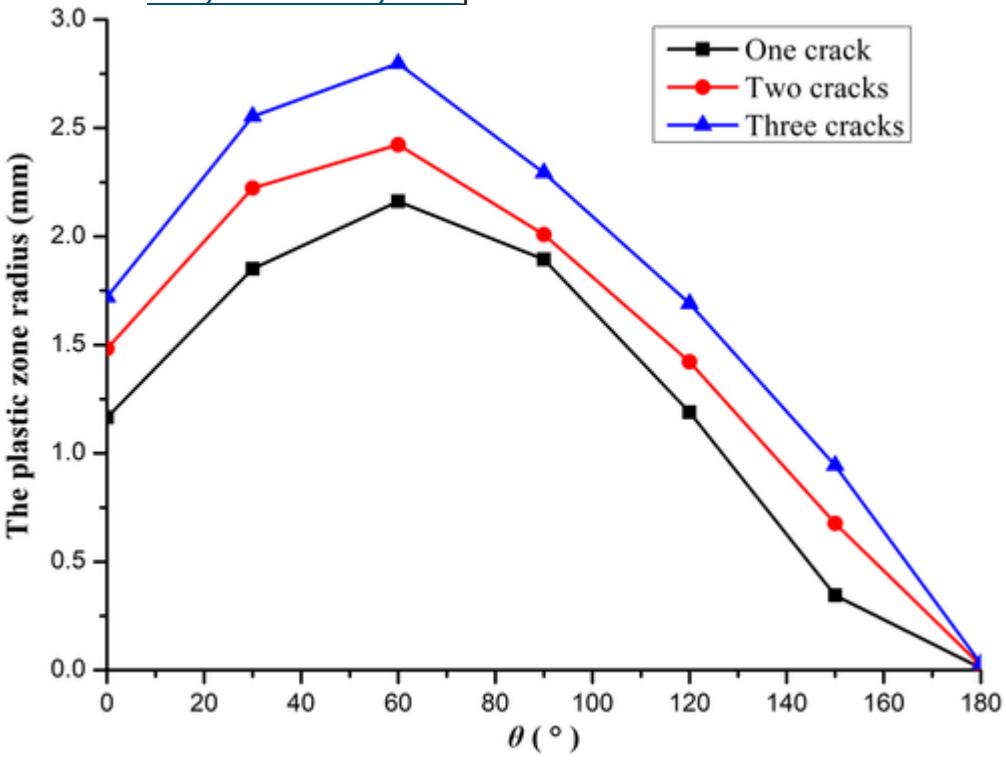

Figure 18

Open in figure viewerPowerPoint
Comparison of the plastic zone radius near the inner tip of crack ② in array of 2 and 3 parallel cracks and single crack with the inclination angle of 135° [Colour figure can be viewed at wileyonlinelibrary.com]

4.6 Prediction of plastic zones around circular crack

There is a rectangular rock sample with the length of 0.10 m and width of 0.05 m containing a circular crack with the radius of 0.005 m. The rectangular rock sample is divided into 200 × 100 = 20 000 discrete nodes. The grid space between adjacent two points is $\Delta x = 5 \times 10^{-4}$ m. The calculation parameters are listed as follows: $\delta = 3\Delta x$, $s_0 = 0.082$, Young's modulus is E = 100GPa, the mass density ρ is 2200 kg/m^3, and Poisson's ratio v is 0.30. Because dynamic analysis is used, the recommended time step 5.33×10^{-8} seconds is specified. Its geometric configuration is plotted in Figure 19. When time step arrives at 370, radius of plastic zone around circular crack is plotted in Figure 20. It can be observed from Figure 20 that the plastic zone around circular crack in the plate under the uniaxial tension is symmetric.

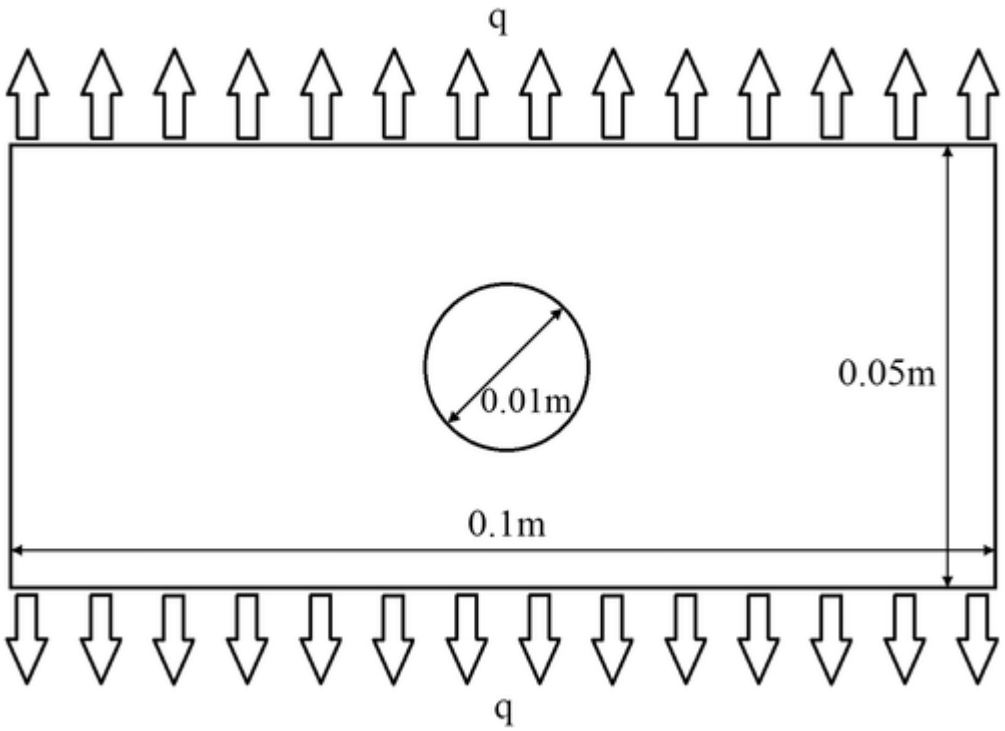

Figure 19
Open in figure viewerPowerPoint
The geometric configure of the rock sample with a circular crack

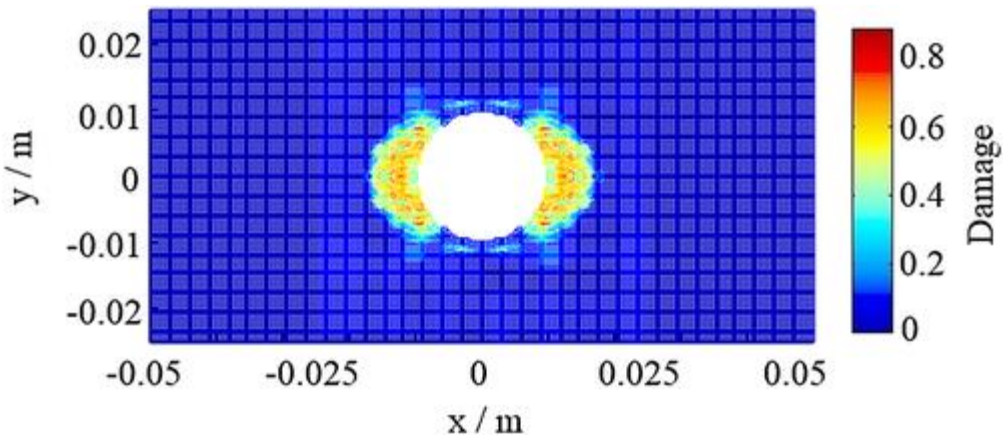

Figure 20
Open in figure viewerPowerPoint
Peridynamic simulation of plastic zone around a circular crack [Colour figure can be viewed at wileyonlinelibrary.com]

5 CONCLUSIONS

The plastic model of ordinary state-based peridynamics is introduced in this paper. The radius of plastic zone near the tips of cracks with the different inclination angles is simulated using ordinary state-based peridynamics. Comparison between the plastic zone radius near the crack tips obtained from peridynamic numerical solution and analytical solution is made. It is found that the relative error between the peridynamic and analytical solution is very little. Therefore, it is feasible to predict the plastic zone near crack tips in rocks using ordinary state-based peridynamics. In the future work, numerical convergence, ie, δ-convergence and m-convergence, of the plastic zone around the crack tips will be investigated. Moreover, the strain hardening plastic model and strain softening plastic model will be implemented into the ordinary state-based peridynamics, and the corresponding characteristics of plastic zones around crack tips in rocks will be analysed.